LETTERS

Golgi maturation visualized in living yeast

Eugene Losev[1], Catherine A. Reinke[1], Jennifer Jellen[1], Daniel E. Strongin[1], Brooke J. Bevis[1] & Benjamin S. Glick[1]

The Golgi apparatus is composed of biochemically distinct early (*cis*, *medial*) and late (*trans*, TGN) cisternae. There is debate about the nature of these cisternae[1–3]. The stable compartments model predicts that each cisterna is a long-lived structure that retains a characteristic set of Golgi-resident proteins. In this view, secretory cargo proteins are transported by vesicles from one cisterna to the next. The cisternal maturation model predicts that each cisterna is a transient structure that matures from early to late by acquiring and then losing specific Golgi-resident proteins. In this view, secretory cargo proteins traverse the Golgi by remaining within the maturing cisternae. Various observations have been interpreted as supporting one or the other mechanism[4–9]. Here we provide a direct test of the two models using three-dimensional time-lapse fluorescence microscopy of the yeast *Saccharomyces cerevisiae*. This approach reveals that individual cisternae mature, and do so at a consistent rate. In parallel, we used pulse–chase analysis to measure the transport of two secretory cargo proteins. The rate of cisternal maturation matches the rate of protein transport through the secretory pathway, suggesting that cisternal maturation can account for the kinetics of secretory traffic.

Our experimental strategy was to visualize individual cisternae and determine whether the composition of Golgi-resident proteins changed over time (Supplementary Fig. S1). According to the stable compartments model, if an early Golgi protein were tagged with green fluorescent protein (GFP), then an early cisterna should exhibit green fluorescence indefinitely. However, according to the cisternal maturation model, an early cisterna should acquire green fluorescence, remain fluorescent for a brief period and then lose fluorescence. A further test would be to tag an early Golgi protein with GFP and a late Golgi protein with DsRed. If Golgi compartments are stable, a given cisterna should stay the same fluorescent colour, but if the compartments are transient, each cisterna should change colour from green to red (Supplementary Movies S1a, b).

Although these experiments are conceptually simple, they are experimentally challenging because light microscopy cannot distinguish individual cisternae in a stacked Golgi. We circumvented this problem using *S. cerevisiae*, in which Golgi cisternae are not stacked and are therefore resolvable by fluorescence microscopy[5,10,11]. Cisternal stacking probably does not affect the basic mode of Golgi operation, because the budding yeast *Pichia pastoris* has a stacked Golgi but resembles *S. cerevisiae* with regards to secretion kinetics and Golgi compartmentation[12,13], and because the secretory machinery is conserved between yeast and mammals[14].

We examined Golgi dynamics at 23 °C using three-dimensional time-lapse confocal microscopy (that is, four-dimensional or 4D microscopy)[15,16]. Every 1–3 s, we captured a *z*-stack of 16–24 optical sections spanning the entire cell. The optical sections for each *z*-stack were then collapsed to generate a 2D projection (Supplementary Fig. S2a). These projections were corrected for photobleaching so that total fluorescence signals remained constant.

The main hurdle was to generate fluorescently tagged Golgi marker proteins that localized correctly at high expression levels without significantly affecting the organelle. Lumenally-oriented Golgi proteins were excluded because GFP folds poorly in the lumen of the yeast secretory pathway[5]. One suitable marker was Sec7, an abundant protein that associates peripherally with late Golgi cisternae[10,17]. Sec7 is concentrated on about half of the cisternae in a cell[13]. The second marker was Vrg4, an abundant transmembrane protein that carries GDP-mannose into the early Golgi[18,19]. Both proteins could be tagged by gene replacement without disrupting their essential functions. Mild (~3-fold) or strong (~12-fold) overexpression of tagged Sec7, or mild (~2-fold) overexpression of tagged Vrg4 had no apparent effect on growth rate (data not shown) or on Golgi compartmentation and secretory pathway activity (Supplementary Figs S3, S4).

When Sec7 or Vrg4 was tagged with GFP, each cell contained multiple fluorescent spots that presumably represented individual Golgi cisternae[5]. These cisternae were mobile and often difficult to follow in the 2D projections. We therefore took advantage of the full 4D data sets, which allowed us to track individual cisternae. For example, Supplementary Movie S2 shows a cisterna being tracked through 20 consecutive *z*-stacks, and Supplementary Fig. S2b shows two cisternae that seem to be connected in a 2D projection but are clearly separate in the corresponding optical sections. Our 4D analysis indicated that cisternal fusion and fission events were uncommon. However, most of the cisternae occasionally passed close enough to other cisternae that they could not be fully resolved even in the optical sections. This problem was exacerbated by the tendency of Golgi cisternae to cluster near sites of polarized growth[11,17]. Each movie ultimately yielded only a few cisternae that could be resolved unambiguously at every time point. We analysed those cisternae quantitatively. As far as we could judge from extensive qualitative observation, most or all cisternae had the same properties as the ones used for quantification.

We first made movies of an *S. cerevisiae* strain expressing a Sec7–GFP fusion protein (Supplementary Movie 1a). To simplify the presentation of relevant data, we also made edited movies showing only the cisternae that were used for quantification (Supplementary Movie 1b). Individual cisternae acquired fluorescence, remained fluorescent for some time and then lost fluorescence (Fig. 1a, b). Analysis of 29 cisternae from a total of ten cells revealed that the duration of labelling with Sec7–GFP was fairly consistent, averaging ~2 min and ranging from about 1 to 3 min (Fig. 1c and Supplementary Table S1). We obtained similar results with a strain expressing GFP–Vrg4 (Supplementary Fig. S5, Supplementary Movie S3a, b and Supplementary Table S1). This transient labelling is consistent with the cisternal maturation model.

Do these marker proteins accurately reflect the dynamics of Golgi cisternae, or do different markers have distinct dynamics? To address this question, we tagged the late Golgi simultaneously with two fluorescent proteins. DsRed-Monomer was fused to Sec7, and GFP was fused to Sys1, a transmembrane protein that recruits the GTPase Arl3 (ref. 20). Sec7–DsRed and Sys1–GFP colocalized extensively (Fig. 2a). Notably, the two proteins often seemed to be partially

[1]Department of Molecular Genetics and Cell Biology, and Institute for Biophysical Dynamics, The University of Chicago, 920 East 58th Street, Chicago, Illinois 60637, USA.

segregated within a given cisterna (Fig. 2c). This observation might indicate the existence of functional domains within cisternae, but might also be an effect of overexpression. In any case, dual-colour 4D imaging confirmed that Sec7–DsRed and Sys1–GFP showed very similar transient labelling of cisternae (Fig. 2b). Two representative cisternae are shown in Fig. 2 and Supplementary Movie 2a, b. In further experiments, GFP was fused to the transmembrane soluble NSF attachment protein receptor (SNARE) Gos1 (refs 15, 21) or the Golgi-localized rhomboid protease Rbd2 (ref. 22). Again, we observed transient labelling of cisternae, although quantification was not performed because GFP–Gos1 overexpression slightly altered the number and size of cisternae, and Rbd2–GFP resulted in some background non-Golgi labelling (data not shown). Thus, we conclude that multiple classes of Golgi proteins share the property of labelling an individual cisterna only transiently.

On the basis of these findings, we attempted to visualize cisternal maturation by simultaneously tagging the early Golgi with GFP–Vrg4 and the late Golgi with Sec7–DsRed. Although the resulting fluorescence patterns were complex, the 4D data sets enabled us to track cisternae that could not always be resolved in the 2D projections (Supplementary Fig. S2c). The results were consistent with a cisternal maturation mechanism. Cisternae exhibited green fluorescence for 2–3 min, then passed through a transition phase when both colours were visible, then exhibited red fluorescence for 2–3 min, and finally lost detectable fluorescence (Fig. 3a). Two representative cisternae are shown in Fig. 3 and Supplementary Movie 3a, b. Red-to-green transitions were never observed. The transition events were often abrupt—for example, the cisternae shown in Fig. 3 lost most of their green fluorescence within 15–20 s. As Vrg4 is present in very early Golgi cisternae[19], whereas Sec7 is present in very late Golgi cisternae[13], the transition phase in which a cisterna contained both fluorescent proteins was brief (Fig. 3b). Each cisterna lost GFP–Vrg4 while acquiring Sec7–DsRed, so the green and red fluoresence signals during the transition phase were low, but both signals were usually visible (Fig. 3c). In four 10-min movies of different cells, we observed a total of 80 green-to-red transitions,

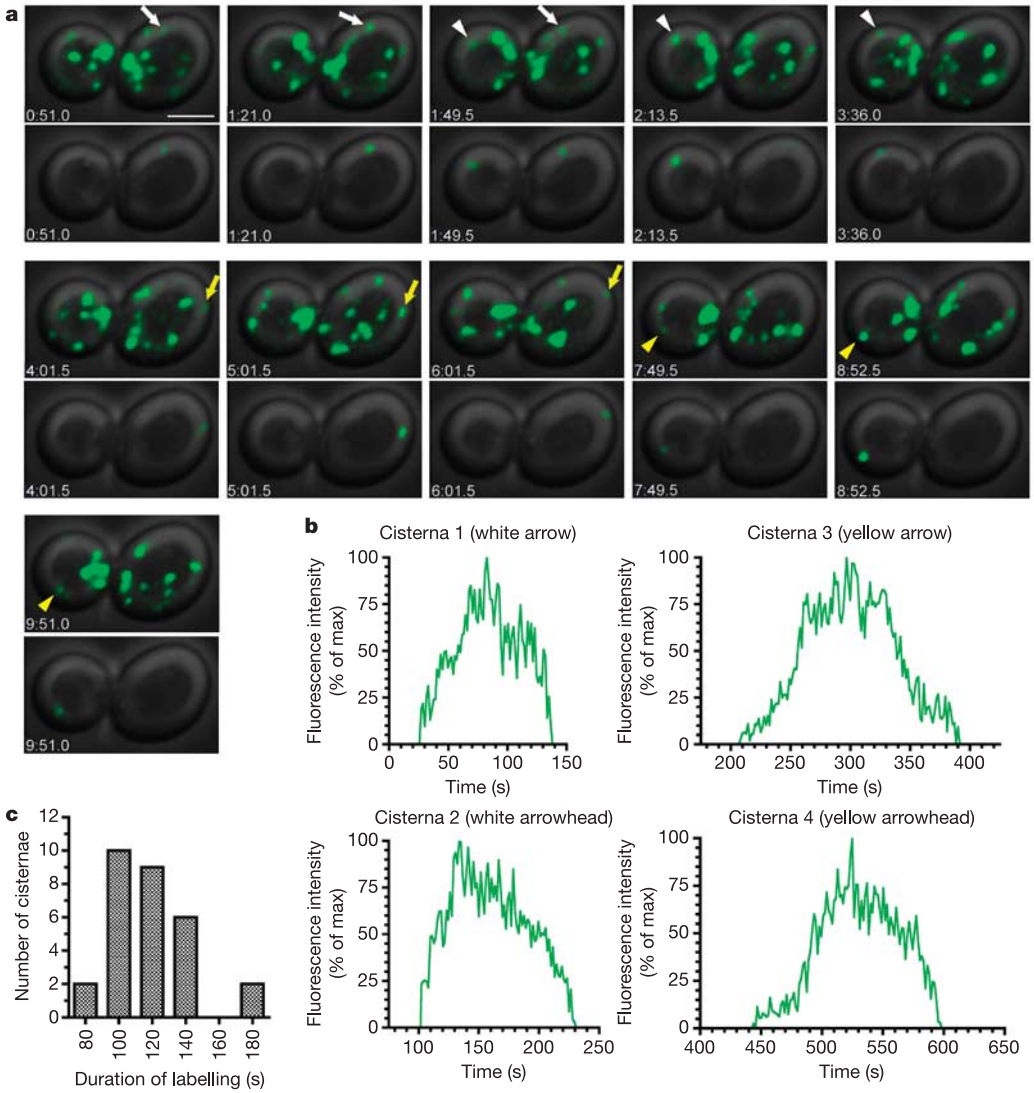

Figure 1 | Sec7–GFP labels each Golgi cisterna for approximately 2 min. **a**, Cropped frames of cells expressing Sec7–GFP from Supplementary Movie 1a, b. Numbers indicate the time (in minutes:seconds) after the movie was initiated. Arrows and arrowheads in the top panels mark four Golgi cisternae that acquired Sec7–GFP fluorescence, increased in brightness and then progressively lost fluorescence. Bottom panels show the same images edited to display only the marked cisternae. Scale bar, 2 μm. **b**, Quantification of data from Supplementary Movie 1b for the cisternae marked in **a**. The horizontal axis indicates the time after the movie was initiated, and the vertical axis indicates Sec7–GFP fluorescence as a percentage of the maximum signal obtained for the designated cisterna. **c**, Histogram showing the distribution of the duration of labelling of cisternae with Sec7–GFP. The durations of detectable fluorescence signals were measured for 29 cisternae from ten independent movies (see Supplementary Table S1).

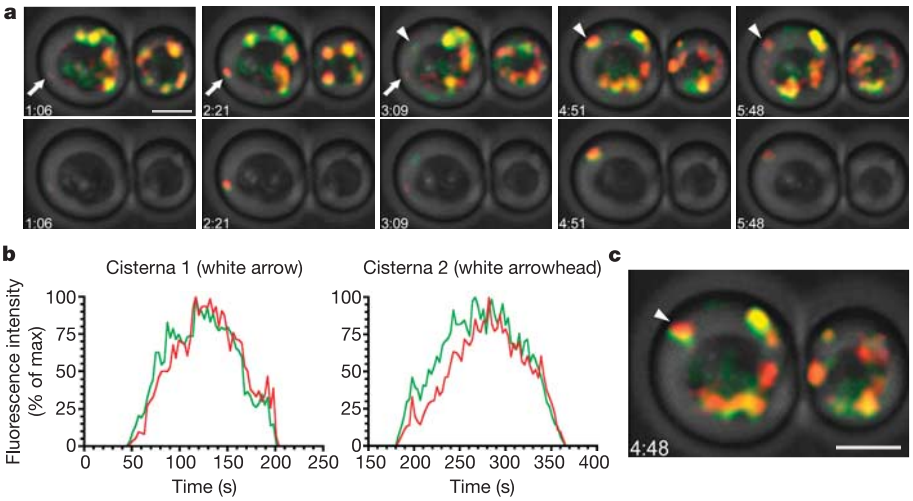

Figure 2 | Two markers of the late Golgi show very similar dynamics. **a**, Cropped frames of cells expressing Sys1–GFP and Sec7–DsRed from Supplementary Movie 2a, b. Data are represented as in Fig. 1a. The arrow and arrowhead mark two Golgi cisternae that acquired Sys1–GFP and Sec7–DsRed fluorescence, transiently displayed fluorescence from both markers and then lost fluorescence from both markers. Scale bar, 2 μm. **b**, Quantification of data from Supplementary Movie 2b. Data are graphed as in Fig. 1b, except that the vertical axis indicates the fluorescence of Sys1–GFP (green) or Sec7–DsRed (red). **c**, Image from Supplementary Movie 2a showing the apparent partial segregation of Sys1–GFP and Sec7–DsRed within the same cisterna. Scale bar, 2 μm.

indicating that most or all cisternae undergo maturation (Supplementary Table S2). Similar results were seen using Sec7–DsRed in conjunction with GFP–Gos1 or Rbd2–GFP, except that the transition phases were longer than with GFP–Vrg4 (data not shown). During all of these transitions, each cisterna seemed to behave autonomously. In summary, each Golgi cisterna showed sequential labelling with GFP–Vrg4 and Sec7–DsRed, for a total of about 4–6 min. The duration of labelling with these two markers presumably represents most or all of the lifetime of a cisterna.

Do these maturation kinetics match the rate of secretory traffic? It has been proposed that cisternal maturation might be too slow to account for the secretion of certain cargo proteins[2]. To address this issue, we performed radioactive pulse–chase measurements with α-factor, which is one of the most rapidly secreted proteins in yeast[23]. Pro-α-factor exists as a 'core' glycoprotein in the endoplasmic reticulum (ER), and is further glycosylated upon reaching the Golgi, where it is cleaved to generate mature α-factor. To resolve ER export from later transport steps, we used a brief 1-min pulse of ^{35}S-Met to create a population of labelled molecules that had entered the secretory pathway at about the same time. A significant fraction of the label was actually incorporated after the chase began, so the starting time point was defined as 30 s into chase. Pro-α-factor reached the Golgi rapidly, with a half-time of ~1 min (Fig. 4a and Supplementary Fig. S6a). Mature α-factor appeared in the extracellular medium with a half-time of ~7 min. Thus, transport from the early Golgi to the extracellular space required ~6 min. If transport of α-factor through the Golgi occurred by cisternal maturation, our videomicroscopy results suggest that intra-Golgi transport

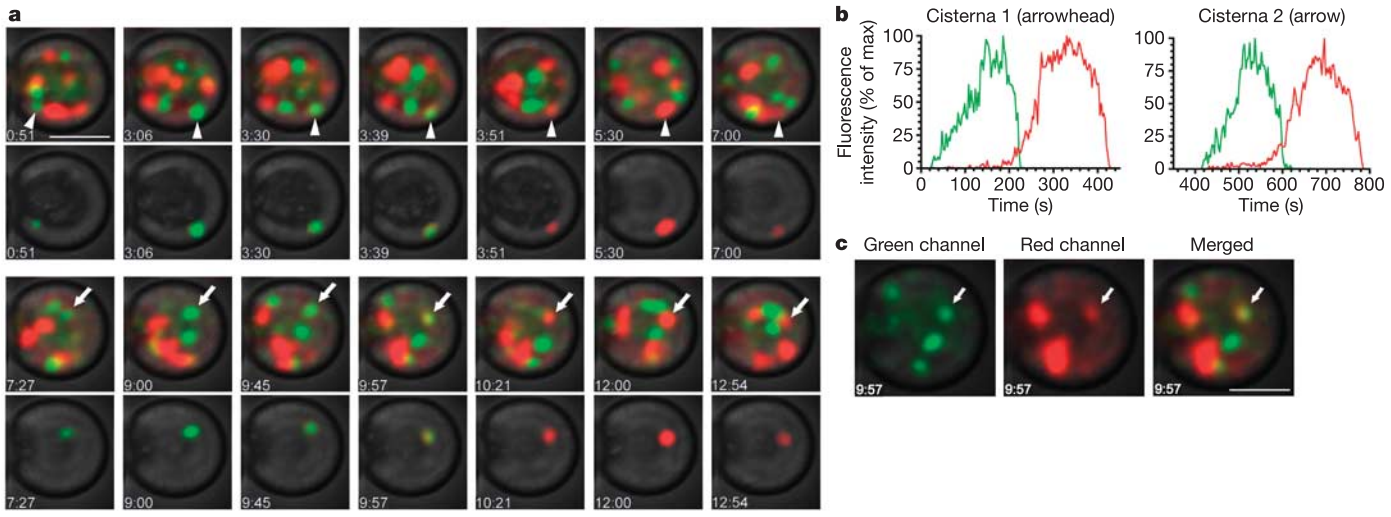

Figure 3 | The resident Golgi protein composition of each cisterna changes over time. **a**, Cropped frames of cells expressing GFP–Vrg4 and Sec7–DsRed from Supplementary Movie 3a, b. Data are represented as in Fig. 1a. The arrow and arrowhead mark two Golgi cisternae that acquired GFP–Vrg4 fluorescence, transiently displayed both GFP–Vrg4 and Sec7–DsRed fluorescence, then displayed exclusively Sec7–DsRed fluorescence and finally lost fluorescence. Scale bar, 2 μm. **b**, Quantification of data from Supplementary Movie 3b. Data are graphed as in Fig. 1b, except that the vertical axis indicates the fluorescence of GFP–Vrg4 (green) or Sec7–DsRed (red). **c**, Example of a cisterna in transition. Green and red channel images for time point 9:57 are shown separately and merged. Scale bar, 2 μm.

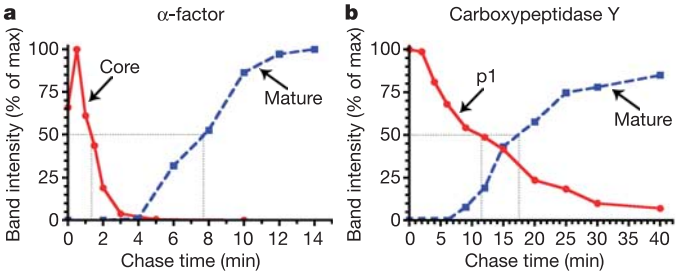

Figure 4 | Secretory pathway transport kinetics are consistent with cisternal maturation. Pulse–chase analysis of α-factor and CPY transport under the growth conditions used for videomicroscopy. See Supplementary Fig. S6 for details. The maximum observed signal for a given protein species was defined as 100%. Dotted lines mark half-times for the appearance and disappearance of the various protein species. **a**, Quantification of α-factor transport. The solid red line represents ER-localized core pro-α-factor, and the dashed blue line represents mature α-factor in the extracellular medium. **b**, Quantification of CPY transport. The solid red line represents ER-localized p1 CPY, and the dashed blue line represents vacuole-localized mature CPY. After 40 min of chase, ~15% of the CPY was still immature, so the maximum value for mature CPY was set at 85%.

required about 4–5 min and Golgi-to-cell-surface transport required an additional 1–2 min. These estimates are consistent with an earlier analysis indicating that pro-α-factor required ~9 min to traverse the Golgi at 15 °C (ref. 23), and with a mammalian cell study indicating that Golgi-to-cell-surface transport is several times faster than intra-Golgi transport[4]. Therefore, our observed rate of cisternal maturation can account for the kinetics of α-factor transport.

We performed similar experiments with carboxypeptidase Y (CPY), which is converted from an ER-localized p1 form to a Golgi-localized p2 form and then to a vacuolar mature form[24]. Because CPY requires some time to fold in the ER, this kinetic analysis was intrinsically less accurate than with α-factor, but was still feasible using a 2-min pulse. CPY moved from the ER to the Golgi with a half-time of ~11.5 min, and from the ER to the vacuole with a half-time of ~17.5 min, implying that transport from the early Golgi to the vacuole required ~6 min (Fig. 4b and Supplementary Fig. S6b). Using the same logic as above, if transport of CPY through the Golgi occurred by cisternal maturation, then intra-Golgi transport required about 4–5 min and Golgi-to-vacuole transport required an additional 1–2 min. In summary, cisternal maturation was somewhat faster than the transport of α-factor or CPY from the early Golgi to the final post-Golgi destination, indicating that cisternal maturation can account for the transport kinetics of these secretory cargo proteins.

Our data, together with findings of a similar study by another group[25], provide direct evidence for the maturation of Golgi cisternae. This conclusion is consistent with earlier analyses of Golgi structure and dynamics in budding yeast[5,13,26–28]. Future experiments will attempt to visualize secretory cargo proteins simultaneously with Golgi-resident proteins, thereby testing the prediction that secretory cargo proteins remain associated with maturing cisternae. A more daunting challenge will be to elucidate the mechanisms of cisternal maturation. Every Golgi-resident protein presumably recycles from older to younger cisternae, but the recycling pathways are likely to vary. Peripheral membrane proteins such as Sec7 might recycle through the cytosol[10]. Some transmembrane Golgi proteins, including certain SNAREs, seem to recycle in COPI vesicles, but there are conflicting reports about whether Golgi glycosylation enzymes enter these vesicles[3]. Studies of mammalian cells have suggested that proteins might move between cisternae via tubular connections[29,30]. Although we have not seen evidence for such connections in *S. cerevisiae*, videomicroscopy is presently unable to reveal whether transmembrane Golgi proteins recycle through small vesicles, larger dissociative transport carriers or inter-cisternal membrane connections. Despite these and many other unresolved questions, the available evidence suggests that in a variety of eukaryotes, cisternal maturation is an important pathway for intra-Golgi transport.

METHODS

Descriptions of yeast strains and plasmids, immunofluorescence and immunoblotting are provided in the Supplementary Information.

Videomicroscopy. *S. cerevisiae* strains were grown to mid-log phase at 23 °C in SD medium, and were imaged under the same conditions. Cells were immobilized on ΔT culture dishes (Bioptechs) using concanavalin A (ref. 15). Single- or dual-colour 4D data sets were collected using a modified LSM 510 confocal microscope (Zeiss), with separate excitation and capture of the red and green fluorescence signals[15,16]. The pixel size was 0.09 μm. For each time point, we collected a stack of optical sections spaced 0.375 μm apart. Typically, 16–24 optical sections were sufficient to span an entire cell. Transmitted light images were stored in the blue channel of RGB TIFF files, and were later converted to grayscale using Adobe Photoshop. Complete *z*-stacks were collected at time points spaced 1.5 s apart (for single-colour imaging) or 3 s apart (for dual-colour imaging). To reduce photodamage, laser illumination was minimized and confocal scans were carried out as quickly as possible.

The 4D data sets were processed essentially as described[15], primarily using custom macros written with NIH Image 1.63 (http://rsb.info.nih.gov/nih-image/). In brief, each optical section was filtered five times with a 3 × 3 hybrid median filter to reduce shot noise. The resulting *z*-stacks were then sharpened by iterative deconvolution using Huygens Essential software (Scientific Volume Imaging). Average intensity projections were corrected for photobleaching. Individual cisternae were tracked manually as follows. At any given time during the analysis, a single *z*-stack of processed optical sections was displayed on the computer screen (see Supplementary Fig. S2). Cisternae of interest were visualized at successive time points by displaying the corresponding *z*-stacks. A cisterna was deemed suitable for quantification if it could be identified in each of a series of consecutive *z*-stacks (as in Supplementary Movie S2), and if it was clearly distinct from the other cisternae at every time point. To make edited movies, optical sections containing the cisternae of interest were selected for projection. Fluorescence signals outside the cisternae of interest were erased using a custom macro. This editing was done either in the 2D projections or in individual optical sections. In the figures, fluorescence signals from the movie frames and screenshots have been slightly enhanced using the 'Levels' command in Photoshop.

Pulse–chase analysis. Pulse–chase experiments were performed essentially as described[31]. Briefly, cells grown at 23 °C in SD medium were transferred to SD medium lacking methionine, and were pulsed with 125 μCi ml^{-1} of Trans^{35}S label (MP Biomedicals). Chases were terminated by adding trichloroacetic acid to a final concentration of 5%. Immunoprecipitations were done using a polyclonal anti-α-factor antibody (a gift from T. Graham) or an anti-CPY antibody (a gift from T. Stevens). Samples were analysed by SDS–PAGE using precast gels (Jule, 16% Tris-Tricine gels for α-factor or 4–16% Tris-glycine gradient gels for CPY). Radioactive bands were visualized using a PhosphorImager and quantified using ImageQuant software (Molecular Dynamics).

Received 20 December 2005; accepted 7 March 2006.
Published online 14 May 2006; corrected 22 June 2006 (details online).

1. Glick, B. S. & Malhotra, V. The curious status of the Golgi apparatus. *Cell* **95**, 883–889 (1998).
2. Pelham, H. R. & Rothman, J. E. The debate about transport in the Golgi—two sides of the same coin? *Cell* **102**, 713–719 (2000).
3. Rabouille, C. & Klumperman, J. Opinion: The maturing role of COPI vesicles in intra-Golgi transport. *Nature Rev. Mol. Cell Biol.* **6**, 812–817 (2005).
4. Bonfanti, L. *et al.* Procollagen traverses the Golgi stack without leaving the lumen of cisternae: evidence for cisternal maturation. *Cell* **95**, 993–1003 (1998).
5. Wooding, S. & Pelham, H. R. B. The dynamics of Golgi protein traffic visualized in living yeast cells. *Mol. Biol. Cell* **9**, 2667–2680 (1998).
6. Volchuk, A. *et al.* Megavesicles implicated in the rapid transport of intracisternal aggregates across the Golgi stack. *Cell* **102**, 335–348 (2000).
7. Mironov, A. A. *et al.* Small cargo proteins and large aggregates can traverse the Golgi by a common mechanism without leaving the lumen of cisternae. *J. Cell Biol.* **155**, 1225–1238 (2001).
8. Martínez-Menárguez, J. A. *et al.* Peri-Golgi vesicles contain retrograde but not anterograde proteins consistent with the cisternal progression model of intra-Golgi transport. *J. Cell Biol.* **155**, 1213–1224 (2001).
9. Cosson, P., Amherdt, M., Rothman, J. E. & Orci, L. A resident Golgi protein is excluded from peri-Golgi vesicles in NRK cells. *Proc. Natl Acad. Sci. USA* **99**, 12831–12834 (2002).

10. Franzusoff, A., Redding, K., Crosby, J., Fuller, R. S. & Schekman, R. Localization of components involved in protein transport and processing through the yeast Golgi apparatus. *J. Cell Biol.* **112,** 27–37 (1991).
11. Preuss, D., Mulholland, J., Franzusoff, A., Segev, N. & Botstein, D. Characterization of the *Saccharomyces* Golgi complex through the cell cycle by immunoelectron microscopy. *Mol. Biol. Cell* **3,** 789–803 (1992).
12. Payne, W. E., Gannon, P. M. & Kaiser, C. A. An inducible acid phosphatase from the yeast *Pichia pastoris*: characterization of the gene and its product. *Gene* **163,** 19–26 (1995).
13. Mogelsvang, S., Gomez-Ospina, N., Soderholm, J., Glick, B. S. & Staehelin, L. A. Tomographic evidence for continuous turnover of Golgi cisternae in *Pichia pastoris*. *Mol. Biol. Cell* **14,** 2277–2291 (2003).
14. Duden, R. & Schekman, R. in *The Golgi Apparatus* (eds Berger, E. G. & Roth, J.) 219–246 (Birkhäuser Verlag, Basel, 1997).
15. Bevis, B. J., Hammond, A. T., Reinke, C. A. & Glick, B. S. *De novo* formation of transitional ER sites and Golgi structures in *Pichia pastoris*. *Nature Cell Biol.* **4,** 750–756 (2002).
16. Hammond, A. T. & Glick, B. S. Raising the speed limits for 4D fluorescence microscopy. *Traffic* **1,** 935–940 (2000).
17. Rossanese, O. W. *et al.* A role for actin, Cdc1p and Myo2p in the inheritance of late Golgi elements in *Saccharomyces cerevisiae*. *J. Cell Biol.* **153,** 47–61 (2001).
18. Dean, N., Zhang, Y. B. & Poster, J. B. The *VRG4* gene is required for GFP-mannose transport into the lumen of the golgi in the yeast, *Saccharomyces cerevisiae*. *J. Biol. Chem.* **272,** 31908–31914 (1997).
19. Abe, M., Noda, Y., Adachi, H. & Yoda, K. Localization of GDP-mannose transporter in the Golgi requires retrieval to the endoplasmic reticulum depending on its cytoplasmic tail and coatomer. *J. Cell Sci.* **117,** 5687–5696 (2004).
20. Behnia, R., Panic, B., Whyte, J. R. & Munro, S. Targeting of the Arf-like GTPase Arl3p to the Golgi requires N-terminal acetylation and the membrane protein Sys1p. *Nature Cell Biol.* **6,** 405–413 (2004).
21. McNew, J. A. *et al.* Gos1p, a *Saccharomyces cerevisiae* SNARE protein involved in Golgi transport. *FEBS Lett.* **435,** 89–95 (1998).
22. Huh, W. K. *et al.* Global analysis of protein localization in budding yeast. *Nature* **425,** 686–691 (2003).
23. Brigance, W. T., Barlowe, C. & Graham, T. R. Organization of the yeast Golgi complex into at least four functionally distinct compartments. *Mol. Biol. Cell* **11,** 171–182 (2000).
24. Horazdovsky, B. F., DeWald, D. B. & Emr, S. D. Protein transport to the yeast vacuole. *Curr. Opin. Cell Biol.* **7,** 544–551 (1995).
25. Matsuura-Tokita, K., Takeuchi, M., Ichihara, A., Mikuriya, K. & Nakano, A. Live imaging of yeast Golgi cisternal maturation. *Nature* advance online publication, doi:10.1038/nature04737 (14 May 2006).
26. Morin-Ganet, M.-N., Rambourg, A., Deitz, S. B., Franzusoff, A. & Képès, F. Morphogenesis and dynamics of the yeast Golgi apparatus. *Traffic* **1,** 56–68 (2000).
27. Todorow, Z., Spang, A., Carmack, E., Yates, J. & Schekman, R. Active recycling of yeast Golgi mannosyltransferase complexes through the endoplasmic reticulum. *Proc. Natl Acad. Sci. USA* **97,** 13643–13648 (2000).
28. Reinke, C. A., Kozik, P. & Glick, B. S. Golgi inheritance in *Saccharomyces cerevisiae* depends on ER inheritance. *Proc. Natl Acad. Sci. USA* **101,** 18018–18023 (2004).
29. Trucco, A. *et al.* Secretory traffic triggers the formation of tubular continuities across Golgi sub-compartments. *Nature Cell Biol.* **6,** 1071–1081 (2004).
30. Marsh, B. J., Volkmann, N., McIntosh, J. R. & Howell, K. E. Direct continuities between cisternae at different levels of the Golgi complex in glucose-stimulated mouse islet beta cells. *Proc. Natl Acad. Sci. USA* **101,** 5565–5570 (2004).
31. Graham, T. R. in *Current Protocols in Cell Biology* (ed. Morgan, K.) 7.6.1–7.6.9 (Wiley, New York, 2000).

Supplementary Information is linked to the online version of the paper at www.nature.com/nature.

Acknowledgements Thanks to A. Franzusoff, T. Stevens and P. Silver for providing reagents, to A. Hammond for advice about microscopy, and to T. Graham for help with pulse–chase analysis. We are grateful to A. Nakano for discussions and for sharing data before publication. This work was supported by grants from the March of Dimes Birth Defects Foundation, the National Institutes of Health and the American Cancer Society.

Author Information Reprints and permissions information is available at npg.nature.com/reprintsandpermissions. The authors declare no competing financial interests. Correspondence and requests for materials should be addressed to B.S.G. (bsglick@midway.uchicago.edu).